

# Space- and time-resolved measurements of temperatures and electron densities of plasmas formed during laser ablation of metallic samples

E.M. Monge, C. Aragón, J.A. Aguilera

Departamento de Física, Universidad Pública de Navarra, Campus de Arrosadía S/N 31006 Pamplona, Spain  
 (Fax: +34-948/169/565, E-mail: carlos.aragon@unavarra.es; j.a.aguilera@unavarra.es)

Received: 21 July 1999/Accepted: 1 September 1999/Published online: 22 December 1999

**Abstract.** Temperature and electron-density profiles in a laser-produced plasma have been measured at various distances from the sample surface and different delay times from the laser pulse. The plasma is produced with a Nd:YAG laser focused on a low-alloy steel sample in air at atmospheric pressure. The determination of the parameters is made starting from the distinct emission spectra emitted by the plasma along a direction parallel to the sample surface and measured simultaneously by a CCD detector. The experimental relative error is 1.5% for temperatures and 4.5% for electron densities. A small spatial variation of the plasma temperature ( $\Delta T \leq 1000$  K) is obtained except for the outer regions, where the intensity is weak. A higher spatial variation is obtained for the electron density, especially at initial times ( $\Delta N_e \cong 10^{17} \text{ cm}^{-3}$  at  $t = 3 \mu\text{s}$ ).

**PACS:** 52.50.Jm; 52.70.Kz

Laser-produced plasmas have become considerably interesting as sources for spectrochemical analysis and measurement of atomic parameters. As is well known, laser plasmas are inhomogeneous and time-dependent sources of radiation. Knowledge of the distribution of temperatures and electron densities in the plasma and their temporal evolution provides information important for laser plasma applications. For example, in elemental analysis using the emission from laser-produced plasmas, Multari et al. [1] found that an improved spectrum with narrower lines can be obtained through spatial masking of the central region of the plasma, where the electron density is higher. Ferrero et al. [2] obtained the distributions of temperature and electron density in a laser plasma and used the plasma parameters in the determination of transition probabilities. This group performed measurements in two perpendicular directions, along the plasma axis, and at right angles to it. In other works, temperatures and electron densities are generally measured only along the plasma axis [3–8]. In our work, two-dimensional distributions of temperatures and electron densities in laser-produced plasmas and their temporal evolution are measured and discussed.

## 1 Experimental set-up

The experimental arrangement is shown in Fig. 1. A Nd:YAG laser (Quantel model Brilliant, wavelength 1064 nm, pulse width 4.5 ns, repetition rate 20 Hz) is focused at right angles to the sample surface by a lens of 150 mm nominal focal length. The sample used is a low-alloy steel. A distance  $d = 135$  mm from the focusing lens to the sample surface has been chosen by taking into account previous work [9], where an increase in the emission-line intensities and plasma stability was demonstrated for a focus placed below the sample surface. The pulse energy is set at 100 mJ by means of an optical attenuator, leading to an estimated power density at the sample surface of  $45 \text{ GW/cm}^2$ . The plasma emission is imaged 1:0.5 on the entrance slit of a spectrometer (Acton Research, model 500 Pro, focal length 0.5 m, 2400 lines/mm grating) by using a lens with a 25-mm diameter and 50-mm focal length. The 50- $\mu\text{m}$  spectrometer slit selects a narrow (0.1-mm wide) vertical region of the plasma emission, whose spectrum is simultaneously recorded with spatial resolution along the  $y$  direction by the CCD detector (EG&G, model

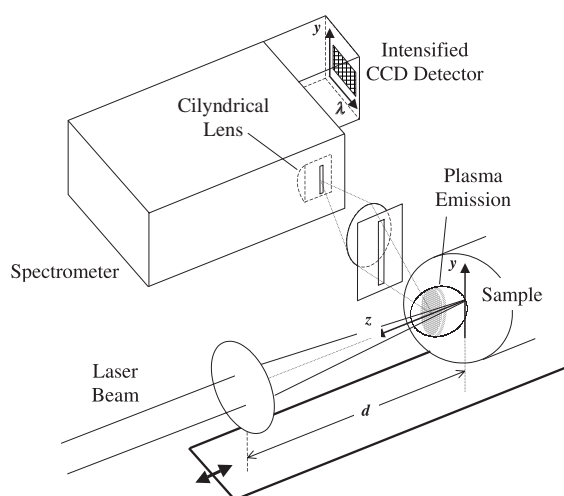


**Fig. 1.** Experimental system for time-resolved measurements of emission-intensity profiles in laser-produced plasmas

OMA IV,  $1024 \times 256$  pixels). A cylindrical lens has been placed inside the spectrometer in order to correct its astigmatism. In order to select the focal length and position of the lens, the focus position of a spectral line emitted by a low-pressure mercury lamp has been observed. A lens with a focal length of 300 mm, separated 36 mm from the input slit, makes the sagittal (imaging) focus of the spectrometer coincide with its tangential (spectral) focus. In this way, the division of the CCD into rows, each with 12 pixels grouped, provides a  $y$ -resolution of 0.45 mm. When the cylindrical lens is used, the shape of the spectral lines is distorted by rays entering the spectrometer at large angles relative to the optical axis. This effect can be minimised if the imaging lens aperture is reduced in the horizontal direction by using a slit, as shown in the figure. In our case, a 1.5-mm wide slit was enough to obtain spectral line profiles similar to those obtained without a cylindrical lens. In order to study the plasma emission at different distances from the sample surface, the sample and focusing lens are fixed to a rail so that they can be displaced in the  $z$  direction with micrometer precision and without modification of the focusing distance. An image intensifier (Princeton Instruments, diameter 18 mm, minimum gate 5 ns) provides time resolution in the detection of the plasma emission. The laser is operated at 20 Hz, but the reading of the CCD takes 380 ms. Thus, a single emission is detected from 8 laser shots, the rest being ignored through an inhibiting signal applied to the intensifier pulse generator. Each acquisition consists in the accumulation of 50 laser shots (20 s, 400 shots in total), and 400 shots previous to accumulation are used to reduce the modification of the crater shape during the measurement.

## 2 Results and discussion

### 2.1 Space- and time-resolved spectra and line-intensity profiles

Figure 2 shows a typical plot of the spectra of the plasma emission as a function of the lateral position  $y$ , for a distance  $z = 1$  mm from the sample surface. A fixed time window of  $1 \mu\text{s}$  and three delays from the laser pulse, at 3, 5 and  $8 \mu\text{s}$ , were used in light detection; the spectra of Fig. 2 correspond to the  $3\text{-}\mu\text{s}$  delay. Note that these spectra have been measured simultaneously by the CCD detector, which significantly reduces the statistical error in the relative intensities obtained. This single spectral region, previously used in [10], is suitable for temperature and electron density measurements in steel plasmas for three reasons. First, it contains Fe emission lines with a large difference between their upper-level energies (about 3.4 eV). Second, it includes the Fe line at 538.34 nm, which has a high Stark broadening parameter, known with precision. Third, high lower-level energies and the moderate transition probability mean the condition of an optically thin plasma is satisfied for these lines. The intensities (areas) and widths (FWHM) of the emission lines were obtained by fitting them to Voigt profiles. The intensity profiles for a distance  $z = 1$  mm from the sample surface, where the maximum intensity is obtained, at three time delays are shown in Fig. 3 for the line at 538.34 nm. The intensity profiles are similar for the other lines. It must be mentioned that, in these lateral profiles, the emission intensity is integrated along the line

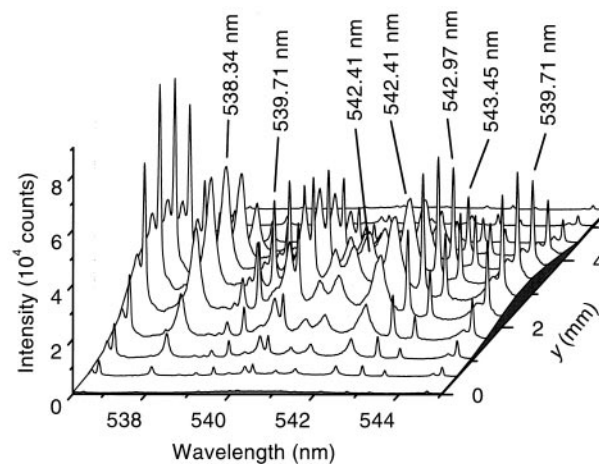


**Fig. 2.** Spectra of the plasma emission as a function of the lateral position  $y$ , for a distance  $z = 1$  mm from the sample surface, at a delay time  $t = 3 \mu\text{s}$  from the laser pulse

of sight ( $x$  direction). We prefer to show the lateral profiles, which result directly from the spectra measured and discuss later the effect of this integration.

### 2.2 Temperature profiles

The values of the plasma temperature were deduced from Boltzmann plots obtained with the measured line intensities, assuming that local thermodynamic equilibrium is present in the plasma. The transition probability values for the neutral iron lines were obtained from [11]. The resulting lateral profiles of the temperature for different distances to the sample surface and delay times are shown in Fig. 4. The error bars represent the typical error value of 1.5% obtained by propagation of the least-squares error in the slope of the Boltzmann plots. The statistical error of the temperature measurements was obtained by performing five measurements in identical conditions, leading to a similar estimation of 1.5%.

In Fig. 4, we can observe that a small variation of the plasma temperature is produced along the lateral position for all the distances  $z$  to the sample surface at all the delay times measured. Only at the edges of the plasma, where

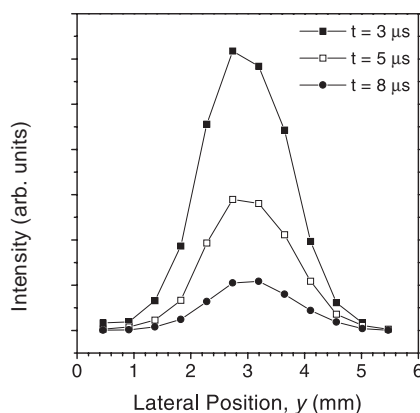


**Fig. 3.** Typical lateral profiles of the intensity of the Fe emission line at 538.34 nm, for a distance  $z = 1$  mm to the sample surface, at different delays from the laser pulse

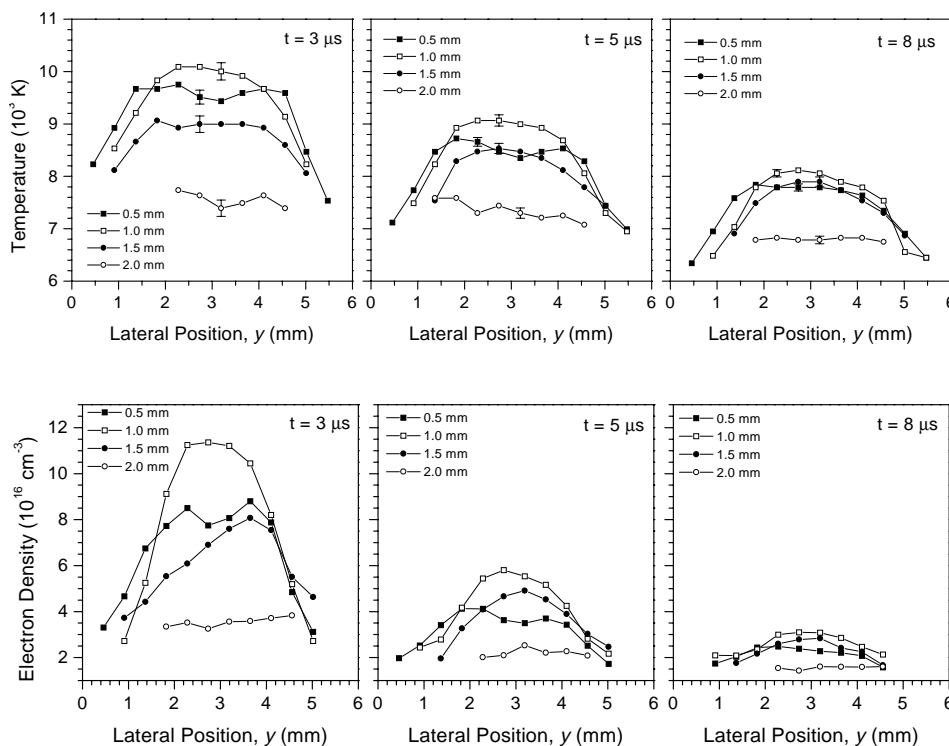


**Fig. 4.** Lateral profiles of the temperature in the plasma for different distances  $z$  from the sample surface at three delay times from the laser pulse

**Fig. 5.** Lateral profiles of the electron density in the plasma for different distances  $z$  from the sample surface at three delay times from the laser pulse

the emission is weak, does the temperature suffer an abrupt drop. This observation agrees with the results obtained by Ferrero et al. [2] for an aluminium-alloy plasma at  $z = 1$  mm and a delay time of  $2 \mu\text{s}$ . In the axial direction, the variation in the temperature is also small in the range of positions  $z = 0.5$ – $1.5$  mm, and again the temperature decreases rapidly at the outer region near  $z = 2$  mm. Similar behaviour for the temperature and axial variation was obtained by Lee et al. [3] for a copper plasma generated in helium at atmospheric pressure by using a Nd:YAG laser. In other works, where the plasmas were also generated at atmospheric pressure but by using excimer lasers [3–6], higher temperatures and a more gradual decrease with the axial distance to the sample surface were obtained.

### 2.3 Electron density profiles

The Stark broadening of the Fe line at  $538.34$  nm has been used to obtain the electron density of the plasma by following the method described by Griem [12]. The Stark broadening parameter for this line is provided in [13, 14] with a 4% relative error. The line width was determined by fitting a Voigt profile. The instrumental width was obtained from emission lines of the plasma, which have small broadening parameters, measured at late times when the electron density is low. Figure 5 shows the lateral profiles of the electron density obtained at different distances  $z$  from the sample surface and delay times from the laser pulse. A cautionary note has to be made about these results. As the electron density increases significantly when the plasma axis is approached, spectra with different line-broadening values are superposed in the  $x$ -integrated spectra. A deconvolution procedure for the line widths is required to correct the electron densities near the axis, which will be carried out in future work. An increase of

20% in the electron density at the axis with respect of the lateral measurement was estimated in [2] for a similar plasma. From the electron densities obtained, the existence of local thermodynamic equilibrium in the plasma can be verified by the criterion described by Thorne [15]. At each position and delay time, the measured electron densities are higher than the critical electron density, which varies from  $5 \times 10^{15} \text{ cm}^{-3}$  to  $7 \times 10^{15} \text{ cm}^{-3}$  for the range of temperatures obtained.

As can be seen in Fig. 5, the electron density has significant spatial variation both in the lateral and in the axial direction. The higher electron density is obtained at all times for a distance  $z = 1$  mm from the sample surface. Also, the plots show that there is a fast temporal decrease in the electron density in the inner region of the plasma.

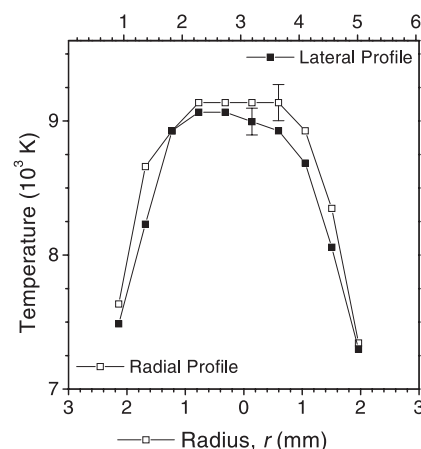


**Fig. 6.** Comparison of the radial profile resulting from the Abel inversion, and the lateral profile of the temperature in the plasma

### 2.4 Abel inversion

In order to convert the measured lateral profiles, in which the emission is integrated in the  $x$  direction, to radial profiles, a deconvolution process has to be carried out. We have studied the effect of this integration in the temperature profile at  $z = 1$  mm,  $t = 5$   $\mu$ s, by performing the deconvolution of the intensity profile by means of the Abel inversion transform, as described by Griem [12]. In Fig. 6, the temperature radial profile resulting from the temperatures calculated with the Abel-transformed intensities is shown together with the lateral profile. As can be seen, the Abel inversion produces only a small correction to the temperature values; this correction is of similar size to the experimental error. This result agrees with the observations made by Ferrero et al. [2].

### 3 Conclusions

We report temperature and electron-density measurements for a laser-produced plasma generated with a steel sample and performed with spatial and temporal resolution by emission spectroscopy. The spectral lines involved in the measurement of both magnitudes are contained in a single spectral region and are detected simultaneously by a CCD, which results in low experimental errors. A weak spatial variation in the tem-

perature has been obtained at the inner region of the plasma, where the major part of the emission is produced.

### References

1. R.A. Multari, L.E. Foster, D.A. Cremers, M.J. Ferris: *Appl. Spectrosc.* **50**, 1483 (1996)
2. F.S. Ferrero, J. Manrique, M. Zwegers, J. Campos: *J. Phys. B* **30**, 893 (1997)
3. Y.-I. Lee, K. Song, H.-K. Cha, J.-M. Lee, M.-C. Park, G.-H. Lee, J. Sneddon: *Appl. Spectrosc.* **51**, 959 (1997)
4. K.J. Grant, G.L. Paul: *Appl. Spectrosc.* **44**, 1349 (1990)
5. Y.-I. Lee, S.P. Sawan, T.L. Thiem, Y.-Y. Teng, J. Sneddon: *Appl. Spectrosc.* **46**, 1597 (1992)
6. Y.-I. Lee, J. Sneddon: *Spectrosc. Lett.* **29**, 1157 (1996)
7. A.H. El-Astal, S. Ikram, T. Morrow, W.G. Graham, D.G. Walmsley: *J. Appl. Phys.* **77**, 6572 (1995)
8. S.S. Harilal, C.V. Bindhu, V.P.N. Nampoori, C.P.G. Vallabhan: *Appl. Spectrosc.* **52**, 449 (1998)
9. J.A. Aguilera, C. Aragón, F. Peñalba: *Appl. Surf. Sci.* **127-129**, 309 (1998)
10. R. Sattmann, V. Sturm, R. Noll: *J. Phys. D: Appl. Phys.* **28**, 2181 (1995)
11. J.R. Fuhr, G.A. Martin, W.L. Wiese, S.M. Younger: *J. Phys. Chem. Ref. Data* **10**, 305 (1981)
12. H.R. Griem: *Plasma Spectroscopy* (McGraw-Hill, New York 1964)
13. N. Konjevic, M.S. Dimitrijevic, W.L. Wiese: *J. Phys. Chem. Ref. Data* **13**, 619 (1984)
14. S. Freudenstein, J. Cooper: *Astron. Astrophys.* **71**, 283 (1979)
15. A.P. Thorne: *Spectrophysics* (Chapman and Hall, New York 1988)